IOP Conference Series: Earth and Environmental Science

PAPER • **OPEN ACCESS**

Validation of CFD analysis of acoustic effects in pump-turbine runners

To cite this article: O Braun *et al* 2019 *IOP Conf. Ser.: Earth Environ. Sci.* **240** 062011

View the article online for updates and enhancements.

This content was downloaded from IP address 159.226.140.26 on 08/10/2019 at 01:29

IOP Conf. Series: Earth and Environmental Science **240** (2019) 062011 doi:10.1088/1755-1315/240/6/062011

Validation of CFD analysis of acoustic effects in pump-turbine runners

O Braun[1] **, B Horisberger**[2] **, N Ruchonnet**[3]**, A Taruffi**[3]**, A Gehrer**[1]

[1] ANDRITZ AG, HPU AS, Stattegger Str. 18, 8045 Graz, Austria
[2] ANDRITZ Hydro AG, Site Investigation & Analysis, Obernauerstrasse 4, 6010 Kriens, Switzerland
[3] ANDRITZ Hydro AG, Turbine Physics, Rue des Deux Gares 6, 1800 Vevey, Switzerland
olivier.braun@andritz.com

Abstract. Rotor-stator interaction is the main cause of harmonic pressure pulsations and resulting dynamic stresses in pump-turbine runners in normal operation. Considering the guide vane passing excitation frequency and the channel length of pump-turbine runners, it shows that compressible effects in the runner channels need to be taken into account for pump-turbines in the medium to high head range. This affects the choice of blade number combinations, the assessment of pressure pulsations and resulting dynamic stresses in components. The compressible effects are primarily linked to the propagation of pressure waves at a finite speed of sound in water. A lower effective wave propagation velocity is sometimes considered to reduce complex fluid-structure interaction effects into simpler pure acoustic problems. In state of the art computational fluid dynamics (CFD) software, using compressible fluid properties allows to reproduce compressibility effects and to combine them with physically accurate transient rotor-stator modelling by sliding interface techniques. The relative motion of the guide vane cascade and the runner is resulting in a periodic variation of the outer channel ends geometry and is also the source of excitation; both effects are thus included in the model which could not be achieved by modal analysis using finite elements. This paper presents the assessment of the prediction capabilities of CFD simulations using commercial software against an experiment carried out on a pump-turbine reduced scale model using air at ambient conditions as a working medium. Using air allows separating the acoustic problem from fluid-structure interaction effects that are not covered in this comparison, and that are intrinsically hard to transpose from model to prototype. The analysis of results focusses on the predicted resonance frequency; its dependency on time step size and number of inner coefficient loops is shown as well as the influence of different model extent and spatial discretization.

1. Introduction

Excitation from rotor-stator interaction is one of the main sources of fatigue for core components of hydraulic machinery. This paper focusses on vibrations in the rotating runner frame, which are excited by the guide vane passing frequency. This topic has been extensively studied; published validation of pressure pulsation amplitudes and induced stresses in the runner is available [1] [2] [3]. Modal and harmonic response analysis using finite element simulations including structural elements representing the runner and acoustic elements representing the water body are state of the art. The prediction of natural frequencies by such an approach is acknowledged to be satisfying for engineering practice and far superior to the former practice of determining natural frequencies of the runner without surrounding medium and applying a corrective factor for the added mass influence of water [4].


Content from this work may be used under the terms of the Creative Commons Attribution 3.0 licence. Any further distribution of this work must maintain attribution to the author(s) and the title of the work, journal citation and DOI.
Published under licence by IOP Publishing Ltd

This former engineering practice reflects the idea of vibration modes being foremost determined by the structural properties of the runner and the water just playing a role in shifting the frequencies by an added-mass effect. This understanding of the nature of runner vibration modes is valid for Francis turbine applications.

As is shown by [5], in pump-turbines the acoustic properties of the water become more important due to the relatively longer blades and resulting longer flow channels in the runner. From a pure fluid mechanics standpoint, neglecting fluid-structure interaction, this relates to standing compression waves in the runner channels. From this fluid mechanics perspective, the elasticity of the structure can be reduced to a shift in effective wave propagation velocity, in a similar way the fluid could be reduced to an added mass effect from a structure mechanics centered viewpoint. In a coupled mechanical system perspective, this results in a possible distinction of two different kinds of natural modes, dominated either by the structural properties or by acoustic properties. In some cases, these modes can certainly interact to a degree where a clear type of a mode is hard to distinguish.

Focusing on the modes dominated by acoustic effects, they can be simulated by computational fluid dynamics (CFD), which allow including the source of excitation and the relative motion of the stationary and rotating frame by sliding interface techniques. Experimentally, pure acoustic modes can clearly be identified in configurations with very stiff and dense structure and highly compressible and low-density fluids, namely in a configuration using air as a working medium with a machine designed for use with water. Fluid-structure interaction effects will become negligible due to the higher density ratio of steel versus air as working medium, so the pure acoustic modes natural frequencies with no relevant shift of wave propagation velocity due to runner elasticity can be obtained from such an experiment. 1-dimensional models of wave interference phenomena in the spiral casing (so called "phase resonance" [4] [6]) of hydraulic turbines were validated in a similar manner by experiments at acoustic similitude using a vacuum cleaner radial fan [7]. These experiments have proven useful in confirming boundary condition assumptions for analytical models [8]. CFD using compressible fluid models was also successfully applied for the simulation of the phase resonance phenomenon [9]. Inspired from the experimental approach of phase resonance investigation [7], the capability of CFD codes to predict resonance conditions in the runner channels is validated with an experiment carried out with a pump turbine scale model using the infrastructure of an IEC-conformal 4-quadrant test rig but changing the working medium to air.

2. Acoustic resonance condition study case

As described in [5], the standing wave that can be encountered in pump-turbine channels is a half wave characterized by the effective channel length L, excited at the guide vane passing frequency $n\,z_0$, (n: speed, z_0: guide vane number). Assuming that pump-turbine relative channel lengths for a given specific speed and runner blade number do not differ drastically, the channel length is characterized by the channel length ratio $\gamma = L/D_1$.

With the wave propagation celerity c, the resonance condition for a standing half wave at resonance speed $n_0$is obtained:

$$n_0\, z_o = \frac{c}{2L} = \frac{c}{2\gamma D_1} \quad or \quad n_0 = \frac{c}{2\gamma D_1 z_0} \tag{1}$$

The guide vane passing frequency depends on the speed, determined to a large extent by the plant layout, and the number of guide vanes. The acoustic resonance frequency depends foremost on the channel length, which is determined mainly by the runner diameter and will only vary slightly within the range of feasible hydraulic designs that fulfill all other criteria. Although constrained by hydraulic and structural design criteria, the choice of blade number combinations is the key parameter to circumvent acoustic resonance in runner channels. From the resonant speed, equation (1), the excitation ratio ν of a pump-turbine rotating at speed n is obtained:

$$\nu = \frac{n}{n_0} = \frac{2n\gamma D_1 z_0}{c} \tag{2}$$

Acoustic similitude is expressed by the circumferential Mach number $Ma_u = \frac{u_1}{c}$. With $u_1 = \pi n D_1$ the relation between excitation ratio ν and circumferential Mach number is obtained:

$$\nu = \frac{2\gamma z_0}{\pi} Ma_u \tag{3}$$

Assuming a wave celerity $c = 1300\, m/s$ as suggested by [5] and a value of 0.7 for the channel length ratio γ, it can be seen that the excitation ratio is far below 1.0 for low head pump turbines and can approach resonant conditions for very high heads. This is obvious from the product nD_1 in the numerator in equation (2), knowing the head of hydraulic turbomachines scales with $(nD)^2$. Such high head turbines will typically have a low specific speed, thus relatively long channels.

Table 1. Circumferential Mach number and excitation ratio estimate for various heads.

Project	**Head [m]**	**Speed [rpm]**	**D1 [m]**	$\mathbf{Z_0}$	$\boldsymbol{Ma_u}$	$\boldsymbol{\nu}$
Tongbai	285	300	4.80	20	0.052	0.48
Feldsee	507	1000	1.91	20	0.07	0.70

3. Experimental setup

A pump-turbine model of low specific speed with $z_2 = 9$ runner blades and $z_0 = 24$ guide vanes with an outer runner diameter $D_1 = 0.548$ m is run in air at ambient conditions. Since fluid-structure interaction effects are negligible, the wave celerity does not differ from the speed of sound: $c = a_0 = 343\, {}^{m}/_{s}$. Resonant conditions from equation (1) assuming $\gamma = 0.7$ are reached for a model speed of ~1000 rpm, equivalent to a resonance circumferential Mach number of $Ma_{u,0} = 0.093$. Running the test rig in a speed range of 700-1300 rpm allows to cover the anticipated range of excitation ratios of ~0.7 to ~1.3.

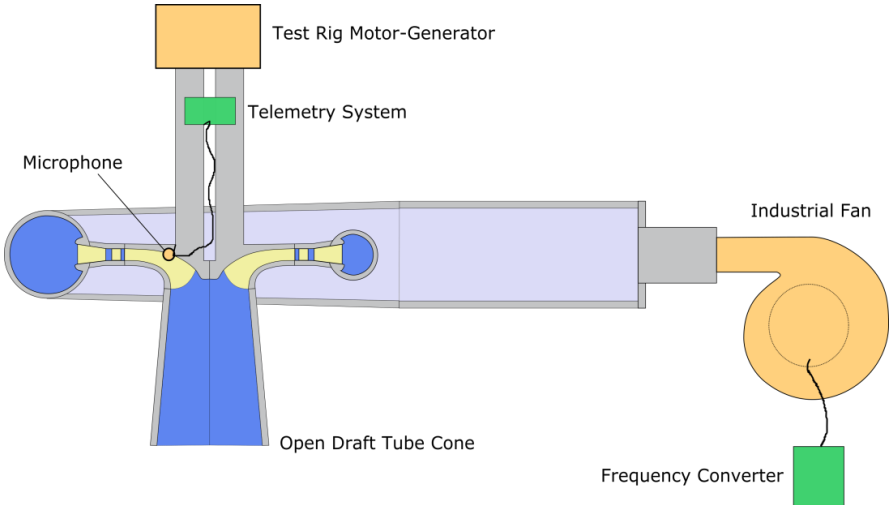


Figure 1. Test setup for acoustic resonance test in air.

The test setup shown in **Figure 1** is run in turbine operation with 16 degrees wicket gate opening and a pressure coefficient based on D_1 of $\psi = 1.1$. The usual closed test rig loop is open at the pressure pipe and the draft tube elbow is removed. An industrial fan with a frequency converter connected to the pressure pipe serves as a booster pump for turbine operation.

The runner is equipped with a pre-polarized surface microphone with a measuring range reaching up to 150dB mounted in a cavity in the hub in the center of the runner channel. The microphone signal is sampled and transmitted to a personal computer by a telemetry system mounted in the shaft assembly at 10kHz acquisition frequency using a low-pass filter with 2kHz cutoff frequency.

4. Numerical model

A commercial finite volume CFD solver (ANSYS CFX 18.1) is used to solve the compressible Navier-Stokes equation implementing a weakly compressible linearized state law for water:

$$\rho = \rho_0 + \frac{(p - p_0)}{c^2} \tag{4}$$

The simulation is carried out using the geometry of the main flow channels of the investigated pump-turbine model, scaled up to a typical prototype scale. By normalizing the results to the circumferential Mach number, the comparison between simulation modeling water at prototype scale and air in the reduced scale experiment is obtained. The simulation domain, represented in **Figure 2**, comprises the spiral case, runner and draft tube cone. The latter is modeled in the rotating domain, so the complexity is reduced to have only one rotating and one stationary component.

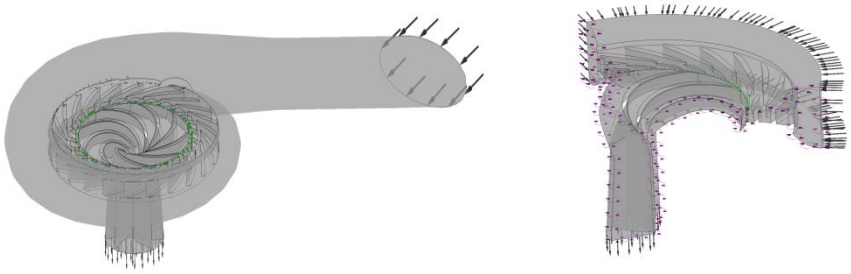


Figure 2. Numerical Simulation Domain, left: full model (SC360), right: reduced domain (Seg120).

A block-structured hexahedral mesh is generated using an in-house tool for the runner flow domain, the distributor domain containing spiral case, stay vane and wicket gate are discretized by a hex-dominant unstructured mesh generated using HExpress Hybrid v.3.2. The second domain extent and spatial discretization variant ("Seg120") only model the guide vanes, stay vanes and a representative average section of spiral casing extruded to a body of revolution. This allows at the same time using only a third of the circumference; fulfilling the periodicity is possible with a 120 degrees segment with the blade number combination of 9/24. For this reduced domain stationary parts, a lightweight but still fine block-structured hexahedral mesh is generated using ICEM CFD.

The outlet at the draft tube cone end is modeled using a standard constant average pressure boundary condition, which has totally reflecting behavior; this is justified for the following reasons:

- It reproduces the experimental setup featuring a sudden expansion to the atmosphere.
- From the phase relationship of waves exiting the runner channels in a nodal diameter 3 pattern, the major part of the acoustic energy is cancelled out in the draft tube cone by superposition of waves, as confirmed by the audible experience on the test rig. No important sound radiation through the open draft tube cone is perceived, this confirms that the acoustic impedance of this boundary does not play a major role.

The inlet condition is placed at a similar length of pressure pipe than implemented in the test, and a standard constant flow rate condition is used where the industrial radial fan blows into the test rig. In order to reduce reflections, an inclined inlet surface is used, spreading the reflection of plane waves over a length equivalent to half the runner diameter. This simplification may affect amplitudes of

pressure waves in the spiral case, but it is assumed that it will not have a major influence on the position of the peak of pulsations in the runner channels which is clearly dominated by runner channel length and excitation frequency by the guide vanes. In case of the reduced domain, the inlet condition is placed on the artificial outer spiral case section.

The simulations are run starting with a steady state solution obtained using a mixing plane interface. The unsteady simulation resolving the relative motion of the domains with a sliding grid approach is initialized from this solution with a time step resolution of 432 time steps per revolution and 5 coefficient loops per time step ("tCoarse"). For the reduced domain extent, a refined time resolution of 1728 time steps per revolution with 7 coefficient loops is applied ("tFine"). The fine simulations are initialized from the transient solution obtained with the coarser time discretization and otherwise identical settings. **Table 2** shows an overview of the different numerical setups.

Table 2. Overview of numerical setups.

Model	**Model Extent**	**SC-Dist Nodes**	**SC-Dist Mesh Type**	**RN Mesh Nodes (per channel)**	**Time steps/ Revolution**	**Coefficient Loops**
SC360-tCoarse	360°(24-9)	7M	unstructured	3M (330k)	432	5
Seg120-tCoarse	120°(8-3)	1.35M	Hex.- Block structured	2M (650k)	432	5
Seg120-tFine	120°(8-3)	1.35M		2M (650k)	1728	7

The convergence level is controlled rather by the limited number of coefficient loops than by a fixed numerical residual threshold value. The level of RMS normed residuals of the momentum reached is 10^{-5} for the coarse and 10^{-6} for the fine time discretization. More important is the achievement of a periodic solution and consistent amplitudes with different settings which is displayed in **Figure 3**.

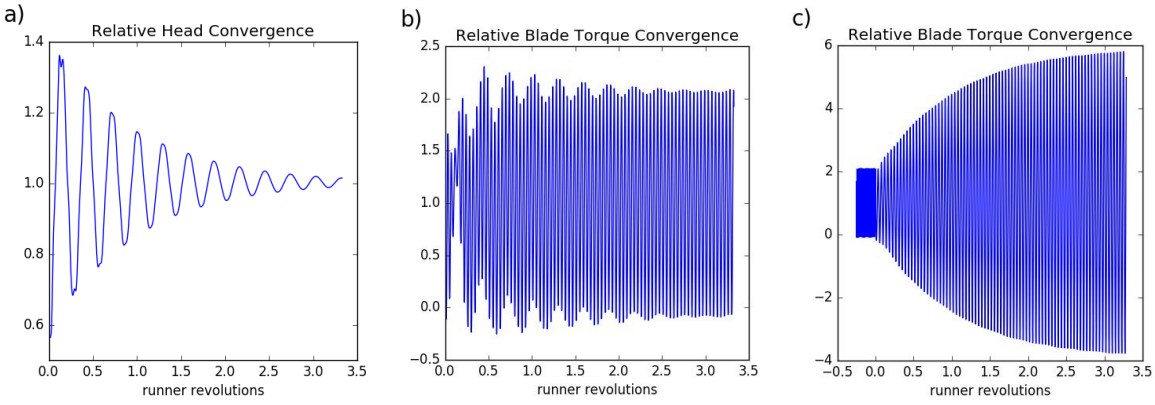


Figure 3. Convergence of numerical simulations. a) Low frequency head pulsations (tCoarse) b) Blade Torque pulsations (tCoarse), c) Blade Torque pulsations after switching to tFine settings.

The left figure shows the evolution of head as a representative of several global quantities, and some decaying low-frequency oscillations are seen, which reflect some long wavelength waves traveling the domain. This undesirable behavior could be cured by using non-reflective conditions. However it is found that the simulation times required to let the oscillation decay are not excessive. The middle plot shows the individual blade torque, a good indicator of integrated pressure pulsations in neighbor channels. It can be seen that the global low-frequency pulsation is reproduced, while the fluctuations at guide vane passing frequency build up in relatively short time and are not overly influenced by the presence of the lower frequency pulsations towards the end of the simulation. Such

uncoupled behavior is expected from a linear system. The right curve shows how the dynamic blade torque evolves after switching from coarse to refined time discretization. For the refined time step setting, convergence to a periodic state takes significantly longer and the resulting amplitudes are higher, which leads to an interpretation of reduced numerical damping. Such numerical damping helps the coarser simulation to reach an asymptotic state with fewer vibration cycles.

Changing speed in the numerical model, as on the test rig, induces a sudden change in operating condition, which would require running through initialization and convergence to periodic state from the beginning. Stepwise variation of circumferential Mach number achieved by changing the fluid properties while letting the operating condition unchanged allows to obtain periodic results in shorter time.

For evaluation of pressure amplitudes, the pressure amplitude at GV passing frequency at the microphone position is evaluated by a Fourier transform, and normalized with a base value at 0 frequency obtained by the fit of an analytic amplitude response curve. The resulting representation is comparable to the textbook response curve of a 1 DOF oscillator. However, the circumferential Mach number is preferred as ordinate to the excitation ratio. The same procedure is applied to the measurement results. **Figure 4** shows the normalized response function with single markers for the individual measurement / simulation points, and lines showing a fit with a 1-DOF amplitude response curve. The free parameters of the fitting are the resonant Mach number, the base amplitude and the damping ratio. The resonant Mach number is marked by a dotted vertical line.

The peak position indicates the measured/predicted resonance circumferential Mach number. Under constant fluid properties, as implemented in the experiment, this represents a variation of rotational speed and thus, excitation frequency. The resonance peak is reached when excitation from guide vane passing reaches the acoustic resonance condition in the runner channel.

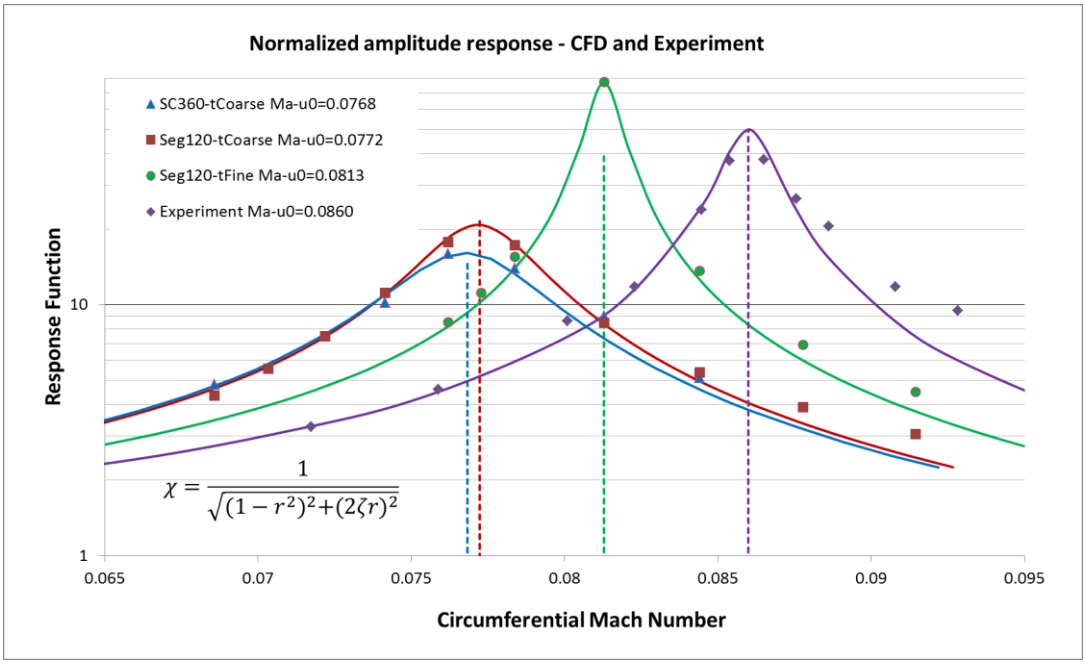


Figure 4. Comparison of response functions from CFD and experiment.

The maximum peak amplitude of the response curve indicates the amplification occurring at resonance and depends on the damping, as measured or as occurring by numerical effects. It needs to be noted that damping of the test setup in air is not expected to give reliable information for the prototype condition.

Both coarse CFD setups show similar results, with an under-prediction of the resonant Mach number of 10% compared to experiment. It is noted that the large domain simulation was only carried out for five different speed of sound values. So the fitting is rather more uncertain than for the reduced domain simulations, but the location of the resonance peak is clearly identified by the two closest simulation points. It can be concluded that the influence of domain extent and mesh refinement on the predicted acoustic resonance frequency in the runner channels is rather low compared to the time step refinement influence.

The CFD simulation with refined time step was run for three values of the speed of sound in the under-critical and three in the over-critical excitation range. The resonant speed of sound was estimated from these six simulations and a seventh simulation was run using this estimated resonant speed of sound value to obtain the peak value on the curve. Noting the logarithmic scaling of the amplitude axis, it can be seen that the numerical damping is sensibly lower than for the coarse time step. The parameters of fitting used to obtain the trend lines in **Figure 4** yield a damping value of 2.4% for the coarse time step settings and 0.65% for the refined time stepping and increased coefficient loop number. This trend to a lower damping and increased amplitudes was also seen for an individual condition for a point being closer to numerical resonance in the refined settings than in the coarse setting. **Figure 3** shows how the refinement of time discretization settings leads directly to a severe increase in fluctuation amplitude.

Generally, the results are well fitted by a simple 1 DOF response curve, except for the higher frequencies, where both experiments and also some of the CFD results show higher amplitudes than a simple 1-DOF assumption. Keeping in mind that we are facing a continuum system, this is not surprising and using a more complex fitting function could certainly improve this situation, but would also require more data to be well supported. However, the position of the main peak of the fitted curve will barely be affected by the use of such an improved fitting.

The overall results of simulations and experiment compared to the estimates used for the design of the experiment show a lower circumferential Mach number for resonant conditions than anticipated. This is due to the fact that the effective length of the blade channel is longer than the rough estimate of $0.7\ D_1$. From basic textbooks treating resonance in simple ducts, it is known that an “end correction” needs to be added to the duct length, and formulae are documented for simple setups such as cylindrical ducts with sudden expansion to open space. In our case, the possible interaction with guide vanes at the runner periphery and the complex inclined shape at the draft tube end make the application of a simple end correction impossible, but the fact that the measured resonant Mach number of 0.086 is below the estimate based on developed channel length corroborates the fact that the effective channel length is longer than a purely geometrical value.

5. Conclusion and Outlook

A resonance peak origination from a purely acoustic half wave standing in runner channels is confirmed by an experiment running a common hydraulic machinery scale model with air as a working medium. The comparison with CFD simulations using water with a linearized compressible state law shows a fair agreement of the predicted position of resonance when represented over circumferential Mach number. While the extent of the domain and mesh resolution and type can be changed without affecting the predicted resonance frequency much, the time discretization (time step size and number of coefficient loops) is a key factor to the predicted resonance frequency and damping. The error in the predicted frequency is reduced from 10% to 5% by using a quarter of the time step size and seven instead of five coefficient loops per time step. The relatively coarse numerical setting that can safely be applied for standard incompressible flow simulations, since rather over-predicting pulsation amplitudes, should not be used in applications aiming to predict compressibility effects, since the position of peak amplitude on the frequency axis is shifted. A more comprehensive study shall implement further refinement of the numerical settings and ascertain the influence of wicket gate opening and flow conditions on the resonance peak position.

References

[1] Coutu A, Proulx D, Colson S and Demers A 2004 Dynamic Assessment of Hydraulic Turbines *Hydro Vision* (Montreal, QC)

[2] Lais S, Liang Q, Henggeler U, Weiss T, Escaler X and Egusquiza E 2008 Dynamic Analysis of Francis Runners: Experiment and Numerical Simulation *IAHR 24th Symp. on Hydraulic Machinery and Systems* (Foz de Iguassu)

[3] Nennemann B, Vu Tand Farhat M 2005 CFD prediction of unsteady wicket-gate runner interaction in Francis turbines: A new standard hydraulic design procedure in *Hydro* (Villach)

[4] Doerfler P, Sick M and Coutu A 2013 *Flow-Induced Pulsation and Vibration in Hydroelectric Machinery* (London: Springer)

[5] Yan J, Koutnik J, Seidel U and Huebner B 2010 Compressible simulation of rotor-stator interaction in pump-turbines *25th IAHR Symp. on Hydraulic Machinery and Systems* (Timisoara)

[6] Doerfler P 1984 On the role of phase resonance in vibrations caused by blade passage in radial hydraulic turbomachines *12 th IAHR Symp.* (Stirling)

[7] Nishiyama Y, Suzuki T, Yonezawa K, Tanaka H, Doerfler P and Tsujimoto Y 2011 Phase Resonance in a Centrifugal Compressor *Int. J. of Fluid Machinery and Systems* **4-3**, 325-33

[8] Ruchonnet N, Taruffi A, Doerfler P and Tsujimoto Y 2013 Phase resonance revisited: The importance of boundary conditions *IAHR Working Group Cavitation and Dynamic Problems in Hydraulic Machinery and Systems* (Ljublijana)

[9] Ruchonnet N, Taruffi A and Braun O 2014 Simulation of Phase Resonance in Radial Hydraulic Machines *18th Int. Sem. on Hydropower Plants* (Vienna)